ELSEVIER

Colloids and Surfaces A: Physicochem. Eng. Aspects 262 (2005) 14–22

COLLOIDS AND SURFACES A

www.elsevier.com/locate/colsurfa

ESEM observations of compacted bentonite submitted to hydration/dehydration conditions

G. Montes-H [a,*], Y. Geraud [b], J. Duplay [a], T. Reuschlé [c]

[a] *UMR 7517 ULP-CNRS, CGS 1, Rue Blessig, F-67084 Strasbourg, France*
[b] *UMR 7516 ULP-EOST, IPG 1, Rue Blessig, F-67084 Strasbourg, France*
[c] *UMR 7516 ULP-EOST, IPG 5, rue de Descartes, F-67084 Strasbourg, France*

Received 24 June 2004; received in revised form 30 March 2005; accepted 31 March 2005
Available online 1 June 2005

Abstract

The MX80 bentonite (bentonite of Wyoming) contains about 85% of montmorillonite and 15% of accessory minerals. The dominant presence of montmorillonite in this clay mineral could cause it to perform exceptionally well as an engineered barrier for a radioactive waste repository because of its swelling properties. In the current study the MX80 bentonite was mechanically compacted by a uniaxial system at four different pressures (21, 35, 49, and 63 MPa) in order to obtain four different physical densities. Then each sample was submitted to a hydration/dehydration cycle into an environmental scanning electron microscopy (ESEM) chamber in order to observe in situ the structural modifications after one hydration/dehydration cycle. This instrument allows the possibility to observe geological samples in their natural state without preliminary preparation or modification. In addition, the classical methods (BET measurements, SEM, Hg-porosimetry and isothermal adsorption of water vapour) were carried out to characterize the texture of compacted samples before hydration/dehydration in the ESEM.

ESEM observations clearly show that the mechanical compaction influences the textural behavior when the bentonite MX80 is submitted to a hydration/dehydration cycle. In general, the inter-aggregate pores are open during hydration stage and sometimes there is an aggregate cracking. This phenomenon is more significant when mechanical compaction increases since the cohesion force of inter-aggregates at high mechanical compaction "49 and 63 MPa" limits the free swelling of MX80 bentonite. In addition, Hg-porosimetry shows that only the macro-porosity (porous size >50 nm) and eventually the meso-porosity (porous size between 2 and 50 nm) are affected by the mechanical compaction. In fact, the total porosity decreases when the mechanical compaction increases. On other hand, BET measurements and adsorption isotherms of water vapour show a non-significant impact on the microporosity.

Keywords: Bentonite; ESEM; Compaction; Texture; Hydration/dehydration; Swelling

1. Introduction

In the municipal, industrial or radioactive wastes storage, an impermeable natural sheet of clay (bentonites) is commonly used as protective barrier in order to avoid the infiltration, lixiviation and/or migration of pollutants [1–5]. Unfortunately, these materials cannot be used in their natural state, because they are heterogeneous, difficult to manipulate or simply because their initial physical density is not sufficient to obtain desirable hydraulic properties. Then, a mechanical conditioning is in general necessary to reach ideal textural properties [6–9].

The textural properties of clay materials depend on the nature of interlayer cations [10–14] and on the layer charge [12]. The mechanical compaction also influences the bentonite's texture, mainly the porous structure. For example, when the mechanical compaction increases, the meso-porosity (porous size between 2 and 50 nm) is lightly affected, the N_2 specific surface area (BET measurements) is constant and only the macro-porosity (porous size >50 nm)

* Corresponding author. Fax: +33 390240402.
E-mail addresses: montes@illite.u-strasbg.fr, german_montes@hotmail.com (G. Montes-H).

0927-7757/$ – see front matter © 2005 Elsevier B.V. All rights reserved.
doi:10.1016/j.colsurfa.2005.03.021

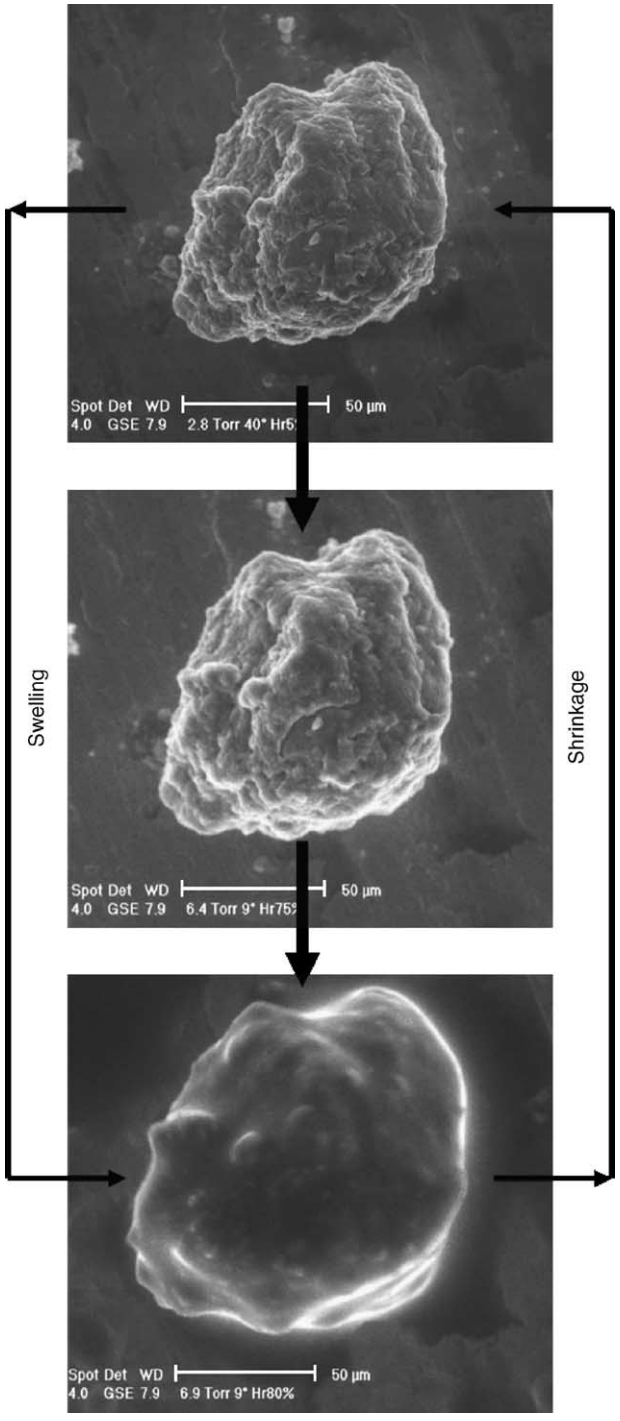

Fig. 1. Swelling–shrinkage property of MX80 bentonite. ESEM (environmental scanning electron microscope) observations [24,20].

decreases since the porous network is generally reorganized according to the "diminution of the total porosity" [6]. Theoretically, a diminution of the soil's total porosity by compaction produces a permeability diminution and thus a minimization of fluid circulation into the porous network [15–18]. However, the bentonites are classified as deformable materials since these materials swell during

Table 1
Mineral composition of the MX80 bentonite

	Proportion (%)	Proportion (%) "without molecular water" drying at 105 °C
Montmorillonite	70.6 ± 2.7	79.2 ± 3.0
Phlogopite 1 M	2.7 ± 2.7	3.0 ± 3.0
Pyrite	0.5	0.6
Calcite	0.7 ± 0.5	0.8 ± 0.6
Ankérite	1.0 ± 0.3	1.1 ± 0.4
Anatase	0.1	0.1
Plagioclase	8.2 ± 2.7	9.2 ± 3.0
Feldspath K	1.8 ± 1.8	2.0 ± 2.0
Phosphate	0.6	0.6
Quartz + cristobalite	2.5 ± 2.5	2.8 ± 2.8
Fe_2O_3	0.4 ± 0.3	0.5 ± 0.4
Molecular water	10.8	–
Organic carbon	0.1	0.1
Total	100	100

ICP-MS and other complementary analysis [6].

hydration and shrink during dehydration (see Fig. 1). This complex phenomenon and the previous observations justify the importance to observe in situ compacted samples of bentonite submitted to hydration/dehydration conditions. For that purpose, a uniaxial system of mechanical compaction was performed in order to obtain four physical densities (1820, 1950, 2030, 2080 kg/m^3). Then each sample was submitted to a hydration/dehydration cycle into an environmental scanning electron microscopy (ESEM) chamber in order to observe in situ the structural modifications after one hydration/dehydration cycle. This instrument allows the possibility to observe geological samples in their natural state without preliminary preparation or modification. In addition, the classical methods (BET measurements, SEM, Hg-porosimetry and isothermal adsorption of water vapour) were carried out to characterize the texture of compacted samples before hydration/dehydration in the ESEM.

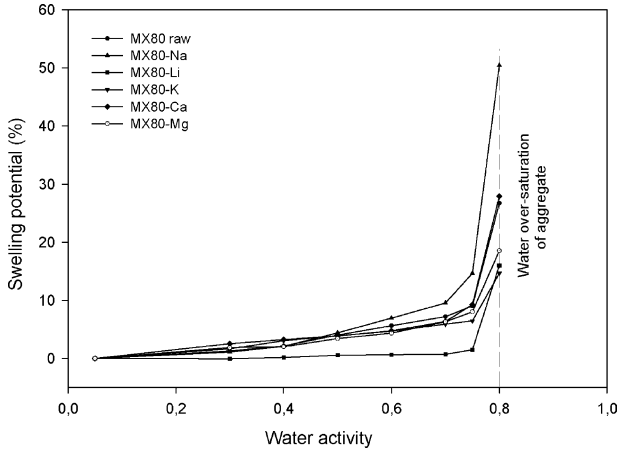

Fig. 2. Swelling isotherms of cation-saturated and natural bentonites by ESEM-DIA [24] "Environmental scanning electron microscopy—digital image analysis". Here, water activity = (RH: relative humidity)/100.

Table 2
Physical characteristics of MX80 bentonite submitted to different mechanical compaction

Sample label	Confining pressure (MPa)	Physical density (kg/m^3)	S_{BET} (m^2/kg)	W (a_w = 0.95) (kg/kg$_{dry\ clay}$)
MX80-21 MPa	21	1820	21230	0.2822
MX80-35 MPa	35	1950	23180	0.2895
MX80-49 MPa	49	2030	22790	0.2896
MX80-63 MPa	63	2080	20370	0.2910

S_{BET}: specific surface area (BET method); W: maximal amount of adsorbed water.

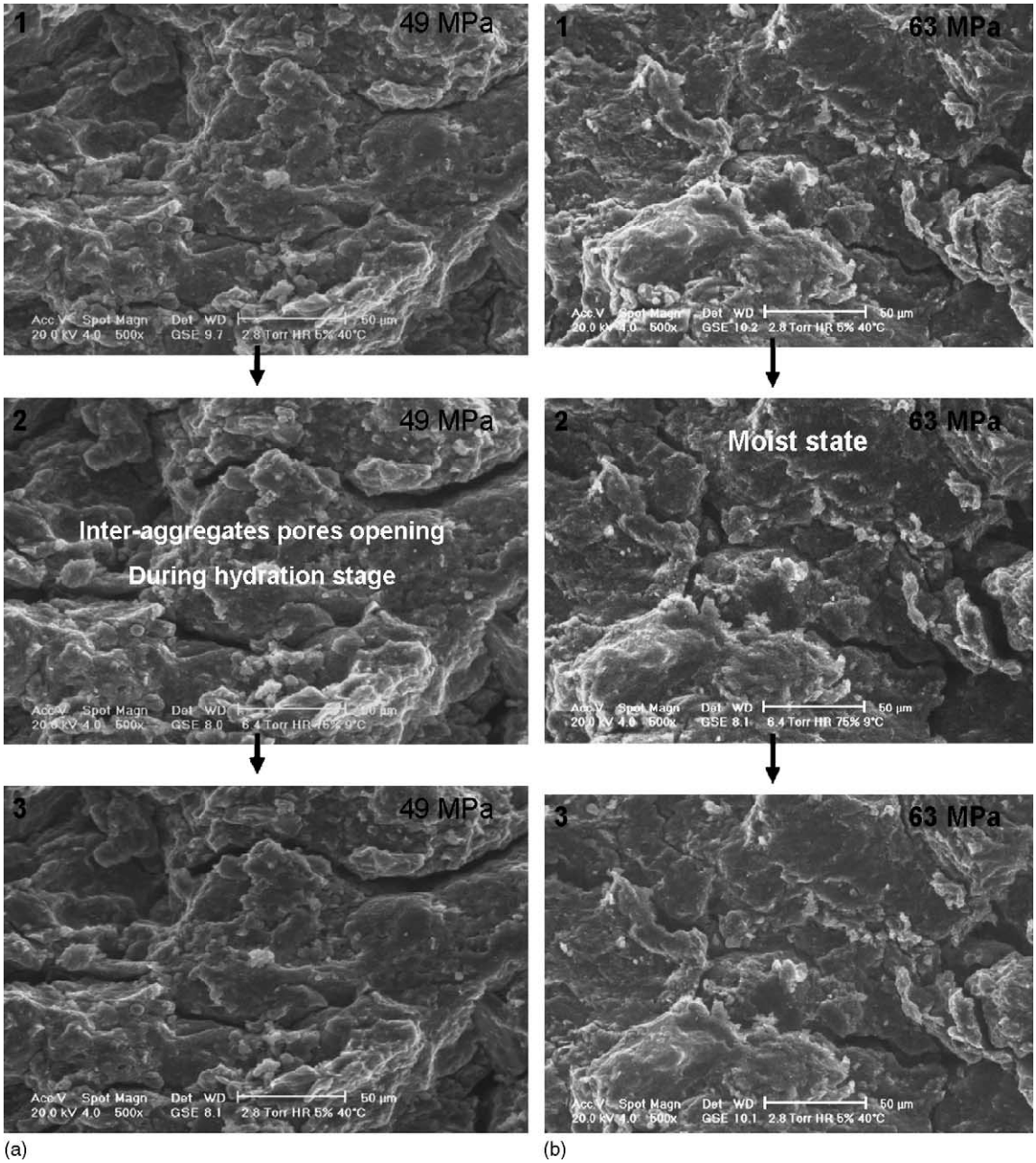

Fig. 3. (a) ESEM micrographs. Opening of inter-aggregates pores after one hydration/dehydration cycle. MX80 bentonite compressed at 49 MPa "MX80-49 MPa sample". (1) Initial state (Hr = 5%), (2) moist state (Hr = 75%), and (3) final state (Hr = 5%). (b) ESEM micrographs. Opening of inter-aggregates pores after one hydration/dehydration cycle. MX80 bentonite compressed at 63 MPa "MX80-49 MPa sample". (1) Initial state (Hr = 5%), (2) moist state (Hr = 75%), and (3) final state (Hr = 5%).

2. Experimental methods

2.1. Bentonite characterization

The classical methods were used to estimate the mineralogy of the MX80 bentonite. In fact the complete characterization was achieved by different French laboratories (LEM-CREGU). The description of each analytical technique is not considered in this study.

XRD analysis was carried out directly on bentonite-raw (minerals identification) and oriented clay fraction "<2 μm" (identification of clay family). A comparative analysis with the X-ray diffractogram corresponding to clay mineral permitted to identify the quartz and the montmorillonite as the main mineral phases. In addition the X-ray diffractogram corresponding to the clay fraction shows that the clay family corresponds to a typical smectite "montmorillonite", since the ethylene glycol test shows a shift of the 12 Å peak up to 17.14 Å. The 12 Å peak is closed up to 9.66 Å when the sample is dried at 490 °C.

The clay fraction morphology and chemical composition were studied by means of STEM and ICP-AES. STEM analysis shows folded particles and turbostratic sheets stacking. The average chemical composition obtained by this method permitted the structural formula estimation:

$$(Si_{3.99}Al_{0.01})(A_{l.5413}Mg_{0.2448}Fe(III)_{0.1893})$$

$$Na_{0.2186}Ca_{0.057}O_{10}(OH)_2$$

This structural formula corresponds to a low charge montmorillonite with mixed "Na–Ca" filling interlayer.

ICP-MS and other complementary analyses for chemical composition were used to estimate the mineral composition of the MX80 bentonite (Table 1).

Finally, ESEM observations showed that the potential swelling depends directly on the relative humidity and on the nature of interlayer cations (see Fig. 2).

2.2. Samples preparation

Four bulk samples were mechanically compressed by a uniaxial system (limit of upward thrust = 50 kN) at different pressures (21, 35, 49 and 63 MPa) in order to obtain four physical densities. The displacement speed during mechanical compaction was kept constant at 5 μm/s on all the samples. The mechanical compaction was realized at atmospheric conditions (room temperature = 20 °C and atmospheric pressure about 1×10^5 Pa). In these conditions, the amount of adsorbed water of the bulk samples was estimated at 0.1151 kg/kg of dry clay, i.e. the initial water content of the clay was 11.5%. However, the water content of compacted samples at same atmospheric conditions was estimated between 10 and 11%. In order to keep constant the hydration state of compacted samples, they were stoked in the plastic desiccators (2 l). Here the water activity of air "into the plastic desiccators" and surrounding samples contained in the glass jar was controlled at 0.55 with an oversaturated salt solution ($Na_2Cr_2O_7$).

On the other hand, each mechanical pressure induced a physical density. Here the physical densities were manually estimated on the cylindrical pastilles. These measures were realized at atmospheric conditions, which mean that the sam-

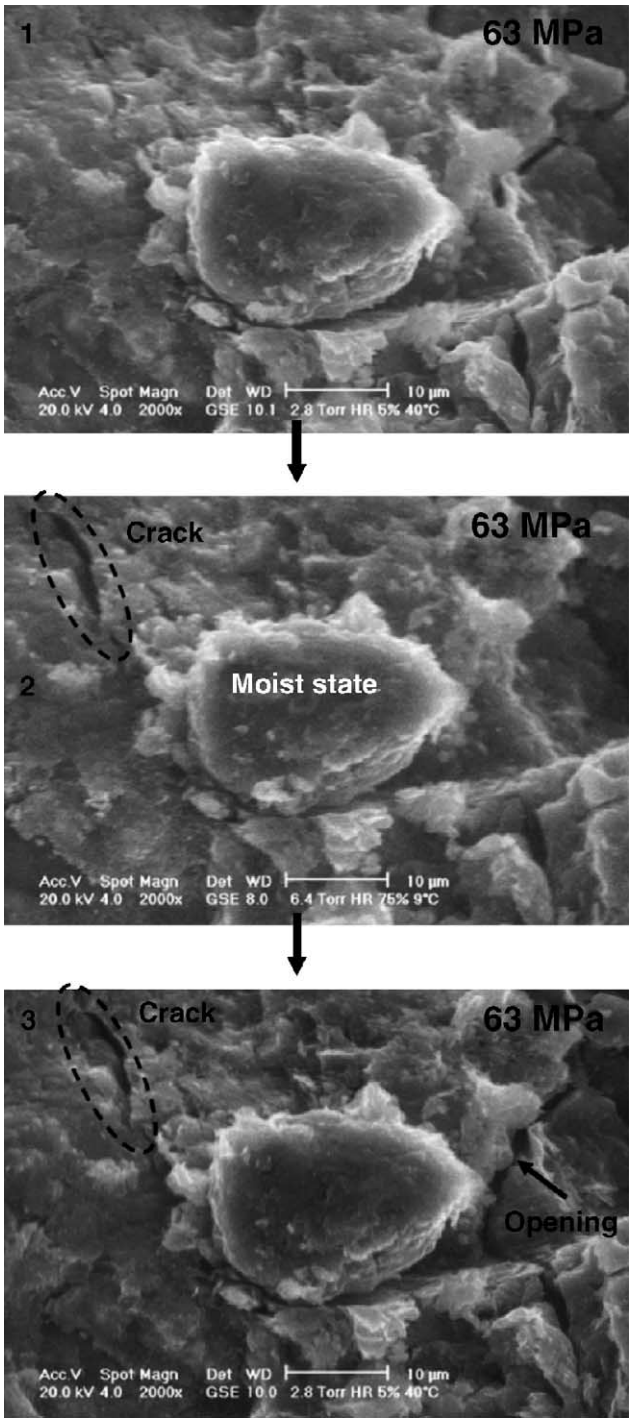

Fig. 4. ESEM micrographs. Aggregate cracking and inter-aggregates opening after one hydration/dehydration cycle. MX80 bentonite compressed at 63 MPa "MX80-63 MPa sample". (1) Initial state (Hr = 5%), (2) moist state (Hr = 75%) and (3) final state (Hr = 5%).

ples were partially hydrated (10–11%). The values estimated are summarized in Table 2.

The total samples used in this paper were labeled as MX80-21, MX80-35, MX80-49 and MX80-63 MPa.

2.3. ESEM methodology

For all ESEM investigations, a XL30 ESEM LaB6 (FEI and Philips) fitted with a gaseous secondary electron detector (GSED) to produce a surface image was used. This microscope is also equipped with a "cooling stage" to control the sample temperature.

The compacted samples were separately submitted to one hydration/dehydration cycle into the ESEM chamber. The hydration/dehydration cycle comprises three stages:

(1) *Drying:* The chamber pressure and sample temperature are respectively set at 373.2 Pa and 40 °C. In this case, the relative moisture of surrounding sample is 5% according to the water phase's diagram. The sample is maintained at these "reference conditions" for about 20 min, and an image of interest is chosen and stored in the hard disk of the control PC "initial state".
(2) *Hydration:* The chamber pressure and the sample temperature are simultaneously set at 853.05 Pa and 9 °C, respectively. Now, the relative moisture of surrounding sample is 75% according to the water phase's diagram. In general, this stage takes approximately 20 min "moist state".
(3) *Dehydration:* Here the chamber pressure and sample temperature are again brought back at reference conditions ($P = 373.2$ Pa and $T = 40$ °C). That is, at 5% of relative moisture of surrounding sample. After 20 min the image of interest was stored again "final state". The samples dimensions were similar for all preparations (4 mm × 4 mm × 2 mm).

The classical methods (BET measurements [13,19]; SEM [20]; Hg-porosimetry [21] and isothermal adsorption of water vapour [14]) were carried out only to characterize the texture of compacted samples before hydration/dehydration in ESEM. The methodology for these methods is not explained in this paper.

3. Results and discussion

3.1. ESEM observations

ESEM observations clearly show that the mechanical compaction influences the textural behavior when the bentonite MX80 is submitted to one hydration/dehydration cycle. In general, the inter-aggregate pores are open during hydration stage "moist state" (see Fig. 3a and b) and sometimes aggregates' cracking appears (Fig. 4). The opening of inter-aggregates' pores and the aggregates' cracking during hydration/dehydration are more significant when mechanical compaction increases since the cohesion force of inter-aggregates at high mechanical compaction limits the free-swelling of MX80 bentonite. For example, a complex cracking as a function of hydration and/or dehydration cycles in the ESEM was observed for a deep argillaceous rock containing dominant swelling-clay (see Fig. 5). However, it is important to remark that in the ESEM chamber is not

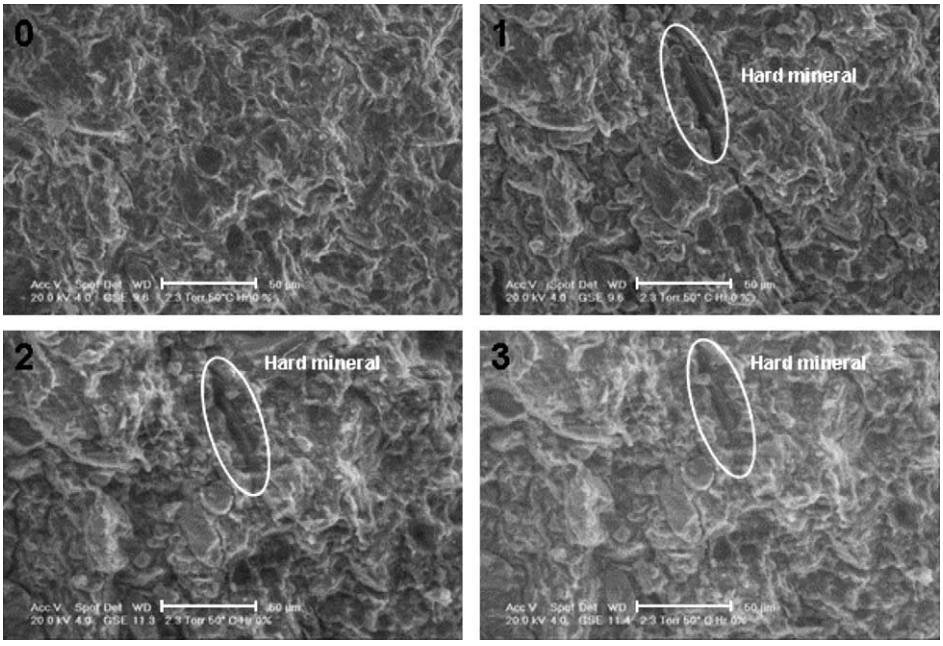

Fig. 5. Complex cracking (partial closing of the cracks) of a deep argillaceous rock "sampling depth = 399 m" as a function of water hydration/dehydration cycles in the ESEM. (0) Initial condition; (1) first cycles; (2) second cycle; (3) third cycle [25].

possible to control the mechanical pressure on the samples (non-constrained samples) then the samples placed into the ESEM chamber expand or shrink freely depending on the relative moisture conditions. In this case, an aggregate deformation could be observed, mainly when the samples are submitted at high relative moisture (>80%).

On the other hand, with moderate pressure of compaction (21 MPa), the MX80-bentonite sample presents an excellent stability after one hydration/dehydration cycle (see Fig. 6).

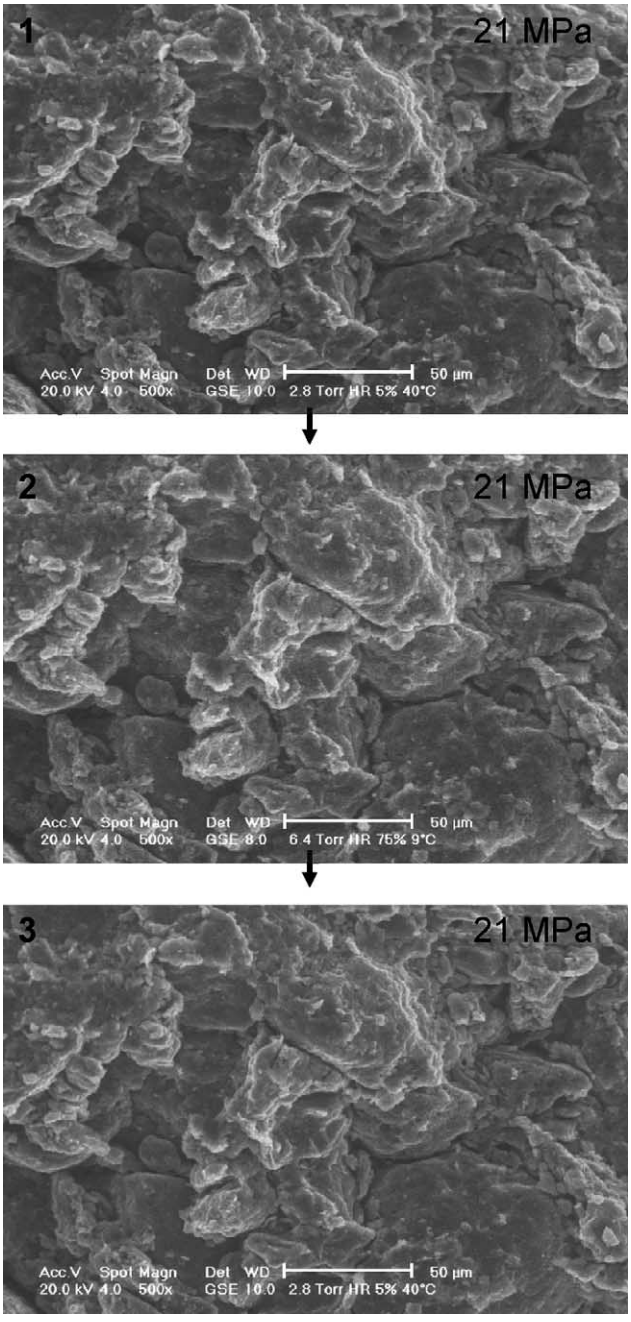

Fig. 6. ESEM micrographs. Excellent stability of porous network "inter-aggregates" after one hydration and dehydration cycle. MX80 bentonite compressed at 21 MPa "MX80-21 MPa sample". (1) Initial state (Hr = 5%), (2) moist state (Hr = 75%), and (3) final state (Hr = 5%).

The microscopy methods are adapted to observe the "short surfaces", for this reason many repetitions of experiments are required in order to obtain a representative elementary surface of a sample (see conclusion).

3.2. Hg-porosimetry and SEM observations

The mercury injection porosimetry shows that only the macro-porosity (porous size >50 nm) and meso-porosity (porous size 2–50 nm) were affected by the mechanical compaction (see Fig. 7a and b). For example, Fig. 7a shows clearly as the pore size distribution is displacing with mechanical compaction intensity. Indeed the total porosity decreases when the physical density increases (Fig. 7b). These results are coherent with literature.

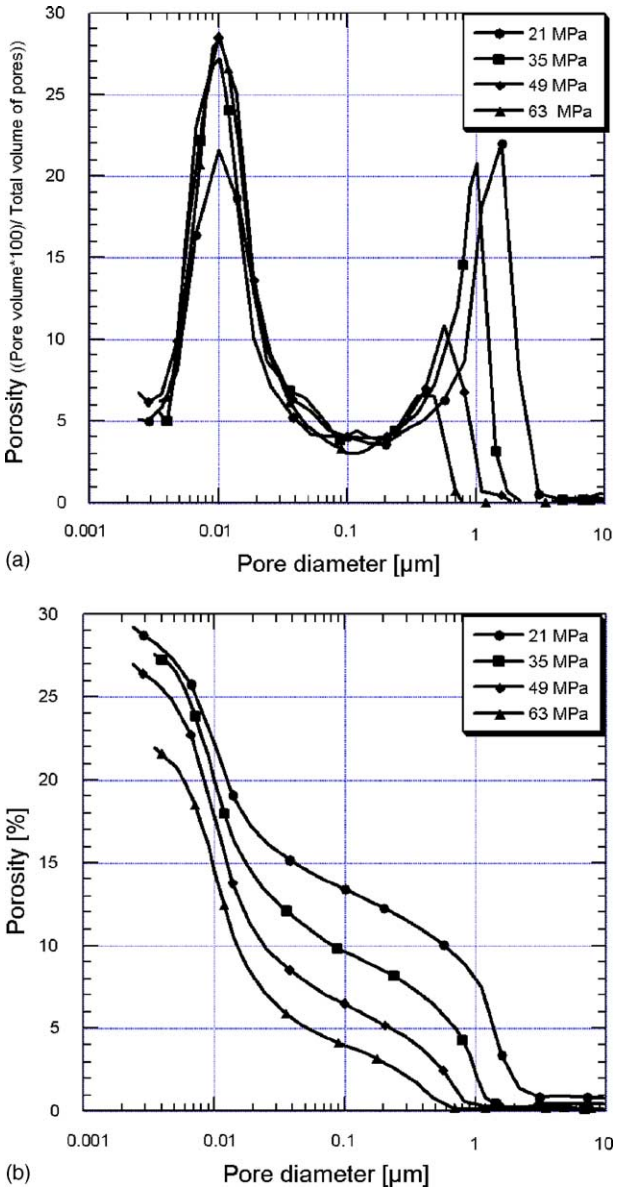

Fig. 7. (a) Pores size distribution to different confining pressure. (b) Total porosity behavior to different confining pressure.

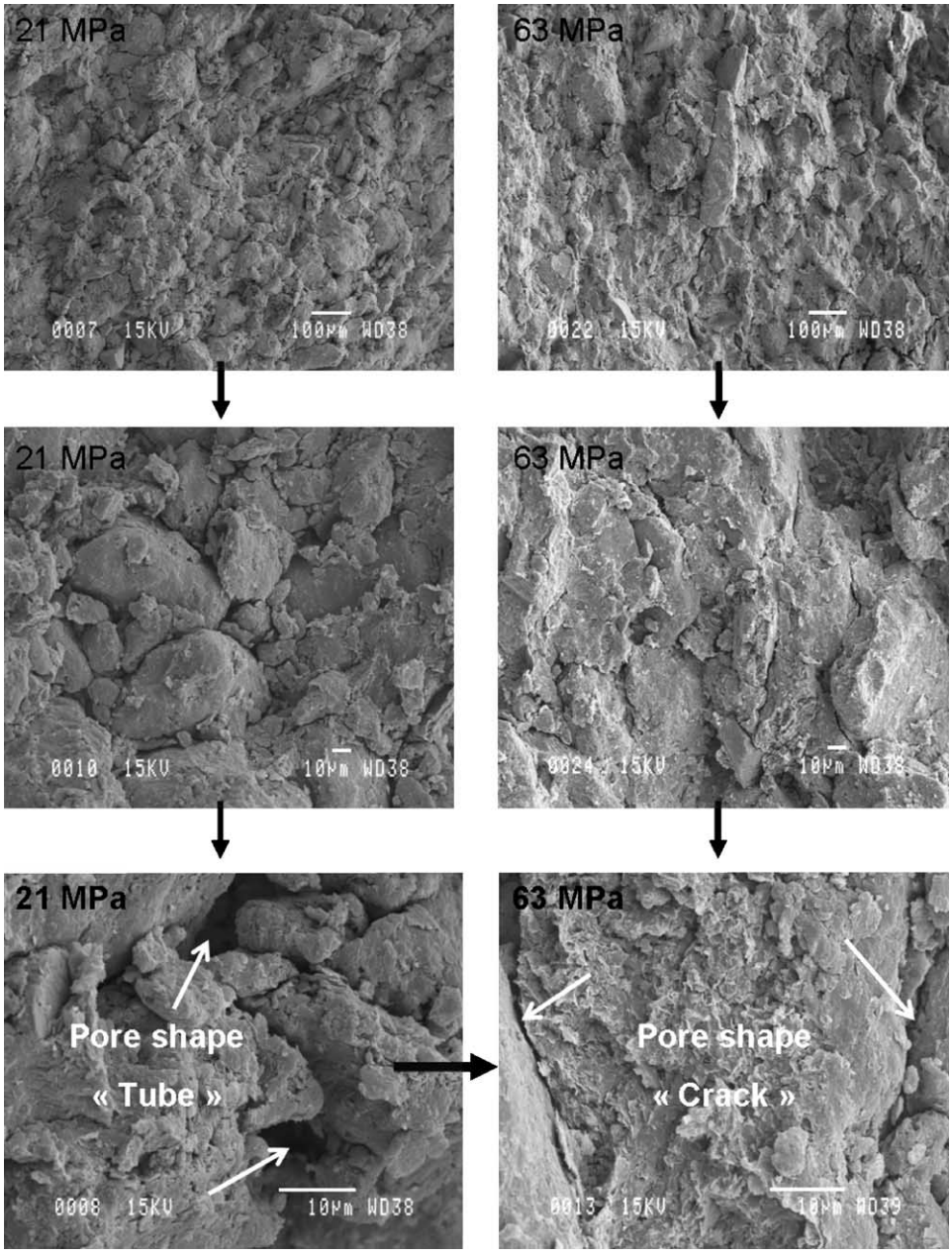

Fig. 8. SEM micrographs. Porous network comparison between a moderate confining pressure (21 MPa) and a high confining pressure (63 MPa) of MX80 bentonite.

SEM observations confirm that the mechanical pressures induce modifications of the inter-aggregate's porous (porous size >5 μm). The macro-pores of the inter-aggregate network present a variation of form, from tubular at moderate pressure of compactions to a system of cracks for high pressure of compaction (see Fig. 8).

3.3. Adsorption isotherms of water vapour and BET measurements

Experimental water adsorption data were fitted by the D'Arcy and Watt equation. This equation considers the monolayer (Langmuir) and multilayer (BET) adsorption [22]. The equation used in terms of water activity "a_w" was

$$W = \frac{w_1 c_1 a_w}{1 + c_1 a_w} + p a_w + \frac{w_M c_M a_w}{1 - c_M} \quad (1)$$

where W is the amount of water adsorbed, w_1 and w_M are the densities of the primary and multilayer adsorption sites, respectively, c_1 and c_M are the interaction parameters related to the heat of adsorption on the primary adsorption sites and in the multilayer, respectively, and p is a constant included in the linear form of the adsorption isotherm.

A computer program (SigmaPlot2000) based on the non-linear least-squares analysis was used for fitting the equation to the water adsorption data. This fitting was only

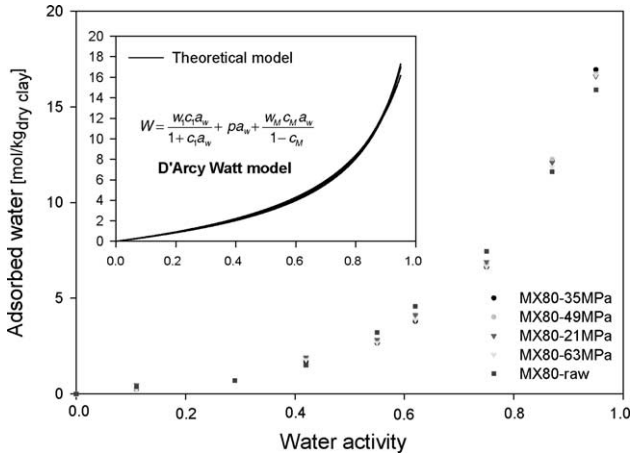

Fig. 9. Adsorption isotherms of water vapour. MX80 bentonite compressed to four confining pressures. Experimental data fitted by D'Arcy–Watt equation.

used to characterize the shape of adsorption–desorption isotherms.

The adsorption isotherms of water vapour at 23 °C are shown in Fig. 9. The shapes of these isotherms seem to correspond to type III of the modern IUPAC classification of isotherms [23]. That is, the isotherms with small solid–fluid interaction at low water activities (<0.5). In contrast, a very high potential of water adsorption was observed at high water activities (>0.5). This may correspond to the formation of water multilayer around the interlayer cation and also to the water capillary condensation.

It is necessary to mention that isotherms III in the IUPAC classification were proposed to describe macro-porous systems. In general, that is not the case for clay minerals. In addition, the interlayer cations play an important role in the water adsorption and swelling. This situation makes a complex mechanism for water adsorption as a function of water activity.

Finally, the adsorption isotherms of water vapour (Fig. 9) shows that the amount of adsorbed water as a function of water activity is not affected with mechanical compaction. In fact, the four water adsorption isotherms are very similar. On the other hand, the BET measurements (Table 2) show that the specific surface area "S_{BET}" is insignificantly affected with the mechanical compaction. This means that the micro-porosity is practically not sensitive to the mechanical compaction.

4. Conclusion

ESEM observations clearly show that the mechanical compaction influences the textural behavior when the bentonite MX80 is submitted to a hydration/dehydration cycle. In general, the inter-aggregate pores are open during hydration stage and sometimes there is an aggregate cracking. This phenomenon is more significant when mechanical compaction increases since the cohesion force of inter-aggregates at high mechanical compaction limits the free swelling of MX80 bentonite. In addition, Hg-porosimetry shows that only the macro-porosity (porous size >50 nm) and eventually the meso-porosity (porous size between 2 and 50 nm) are affected by the mechanical compaction. In fact, the total porosity decreases when the mechanical compaction increases. In this case, SEM observations show a transformation of the shape of the macro-pores network from tube to crack. On other hand, BET measurements and adsorption isotherms of water vapour show that micro-porosity remains practically intact.

Evidently, the ESEM is a powerful tool to observe in situ the hydration and/or dehydration of clays and clay minerals in their natural state. The main advantage of this method is the speed with which one obtains the qualitative and quantitative results. However, this method presents several limitations:

- The hydration/dehydration experiments were carried out under ESEM-chamber pressure (between 13.328 and 1332.8 Pa). This allows only the ability to observe the inter-aggregates opening or aggregates cracking on the non-constrained samples.
- The hydration/dehydration experiments were limited at 80% of relative humidity for swelling clays (powders and compacted powders). In this case, a water over-saturation of surface was observed in consequent the quality of images is poor.
- The ESEM images comprise a very short surface of analysis. For that, it is primordial to make many repetitions of experiments in order to have a good certitude of observations. The results presented in this paper were based only on three repetitive experiments.

In conclusion, the ESEM observations must be considered with care for any civil application.

Acknowledgements

The authors are grateful to National Council of Science and Technology (CONACYT), Mexico, and Louis Pasteur University, France, for providing a financial grant for this work.

References

[1] R. Pusch, Use of bentonite for isolation of radioactive waste products, Clay Miner. 27 (1992) 353–361.
[2] H.H. Murray, Traditional and new applications for kaolin, smectite, and palygorskite: a general overview, Appl. Clay Sci. 17 (2000) 207–221.
[3] D. Koch, Bentonites as a basic material for technical base liners and site encapsulation cut-off walls, Appl. Clay Sci. 21 (2002) 1–11.
[4] C. Benson, D. Daniel, G. Boutwell, Field performance of compacted clays liners, J. Geotech. Geoenviron. Eng., ASCE 125 (5) (1999) 390–403.

[5] D. Daniel, Earthen liners for land disposal facilities, in: R.D. Woods (Ed.), Geotechnical Practice for Waste Disposal'87, GSP No. 13, ASCE, 1987, pp. 21–39.
[6] E. Sauzeat, D. Guillaume, A. Neaman, J. Dubessy, M. François, C. Pfeiffert, M. Pelletier, R. Ruch, O. Barres, J. Yvon, F. Villéras, M. Cathelineau, Caractérisation minéralogique, cristallochimique et texturale de l'argile MX80, Rapport ANDRA No. CRP0ENG 01-001, 2001, 82 pp.
[7] B. Wiebe, J. Graham, G. Xiangmin Tang, D. Dixon, Influence of pressure, saturation and temperature on the behavior of unsaturated sand-bentonite, Can. Geotech. J. 35 (1998) 194–205.
[8] D. Daniel, C. Benson, Water content-density criteria for compacted soils liners, J. Geotech. Eng., ASCE 116 (12) (1990) 1811–1830.
[9] S. Day, D. Daniels, Hydraulic conductivity of two prototype clay liners, J. Geotech. Eng., ASCE 111 (8) (1985) 957–970.
[10] J.M. Cases, I. Berend, G. Besson, M. François, J.P. Uriot, F. Thomas, J.E. Poirier, Mechanism of adsorption and desorption of water vapour by homoionic montmorillonite. I. The sodium exchange form, Langmuir 8 (1992) 2730–2739.
[11] J.M. Cases, I. Berend, M. François, J.P. Uriot, L.J. Michot, F. Thomas, Mechanism of adsorption and desorption of water vapour by homoionic montmorillonite. 3. The Mg^{2+}, Ca^{2+}, Sr^{2+} and Ba^{+2} exchanged forms, Clays Clay Miner. 45 (1997) 8–22.
[12] D.W. Rutherford, Effects of exchanged cation on the micro-porosity of montmorillonite, Clays Clay Miner. 45 (4) (1997) 534–543.
[13] A. Neaman, M. Pelletier, F. Villieras, The effects of exchanged cations, compression, heating and hydration on textural properties of bulk bentonite and its corresponding purified montmorillonite, Appl. Clay Sci. 22 (2003) 153–168.
[14] G. Montes-H, J. Duplay, L. Martinez, Y. Geraud, B. Rousset-Tournier, Influence of interlayer cations on the water sorption and swelling–shrinkage of MX80 bentonite, Appl. Clay Sci. 23 (2003) 309–321.
[15] K. Çarman, Compaction characteristics of towed wheels on clay loam in a soil bin, Soil Till. Res. 65 (2002) 37–43.
[16] D. Jégou, J. Brunotte, H. Rogasik, Y. Capowiez, H. Diestel, S. Schrader, D. Cluzeau, Impact soil compaction on earthworm burrow systems using X-ray computed tomography: preliminary study, Eur. J. Soil Biol. 38 (2002) 329–336.
[17] D.J. McQueen, T.G. Shepherd, Physical changes and compaction sensitivity on a fine-textured, poorly drained soil (Typic Endoaquept) under varying durations of cropping, Manawatu region, New Zealand, Soil Till. Res. 63 (2002) 93–107.
[18] L.F. Pires, J.R. de Macedo, M.D. de Souza, O.O.S Bacchi, K. Reichardt, Gamma-ray computed tomography to investigate compaction on sewage-sludge-treated soil, Appl. Radiat. Isotopes 59 (2003) 17–25.
[19] F. Villiéras, R. Leboda, B. Charmas, F. Bardot, G. Gérard, W. Rudzinski, High resolution argon and nitrogen adsorption assessment of the surface heterogeneity of carbosils, Carbon 36 (10) (1998) 1501–1510.
[20] G. Montes-H, Etude expérimentale de la sorption d'eau et du gonflement des argiles par microscopie électronique à balayage environnementale (ESEM) et analyse digitale d'images, Ph.D. Thesis, Louis Pasteur University, Strasbourg I, France, 2002, 151 pp.
[21] Y. Géraud, J.-M. Caron, P. Faure, Porosity network of a ductile shear zone, J. Struct. Geol. 17 (12) (1995) 1757–1769.
[22] M. Sychev, R. Prohod'ko, A. Stepanenko, M. Rozwadowski, V.H.J. San de Beer, R.A. Van Sarten, Characterization of the micro-porosity of chromia- and titania-pillared montmorillonites differing in pillar density. II. Adsorption of benzene and water, Micropor. Mesopor. Mater. 47 (2001) 311–321.
[23] G. Aranovich, M.D. Donohue, Adsorption hysteresis in porous solids, J. Colloid Interf. Sci. 205 (1998) 121–130.
[24] G. Montes-H, J. Duplay, L. Martinez, C. Mendoza, Swelling–shrinkage kinetics of MX80 bentonite, Appl. Clay Sci. 22 (2003) 279–293.
[25] H.G. Montes, J. Duplay, L. Martinez, S. Escoffier, D. Rousset, Structural modification of Callovo-oxfordian argillite under hydration/dehydration conditions, Appl. Clay Sci. 25 (2004) 187–194.